Mechanical Properties of Porous β-Tricalcium Phosphate Composites Prepared by Ice-Templating and Poly(ε-caprolactone) Impregnation

Stefan Flauder,* Roman Sajzew, and Frank A. Müller

Otto Schott Institute of Materials Research (OSIM), Friedrich Schiller University of Jena, Löbdergraben 32, 07743 Jena, Germany

S *Supporting Information*

ABSTRACT: In this study ceramic scaffolds of the bioresorbable and osteoconductive bioceramic β-tricalcium phosphate (β-TCP) were impregnated with the bioresorbable and ductile polymer poly(ε-caprolactone) (PCL) to investigate the influence of the impregnation on the mechanical properties of the porous composites. The initial β-TCP scaffolds were fabricated by the ice-templating method and exhibit the typical morphology of aligned, open, and lamellar pores. This pore morphology seems to be appropriate for applications as bone replacement material. The macroporosity of the scaffolds is mostly preserved during the solution-mediated PCL impregnation as the polymer was added only in small amounts so that only the micropores of β-TCP lamellae were infiltrated and the surface of the lamellae were coated with a thin film. Composite scaffolds show a failure behavior with brittle and plastic contributions, which increase their damage tolerance, in contrast to the absolutely brittle behavior of pure β-TCP scaffolds. The energy consumption during bending and compression load was increased in the impregnated scaffolds by (a) elastic and plastic deformation of the introduced polymer, (b) drawing and formation of PCL fibrils which bridge micro- and macrocracks, and (c) friction of ceramic debris still glued together by PCL. PCL addition also increased the compressive and flexural strength of the scaffolds. An explanatory model for this strength enhancement was proposed that implicates the stiffening of cold-drawn PCL present in surface flaws and micropores.

KEYWORDS: *porous composites, mechanical properties, ice-templating, β-TCP, polymer impregnation*
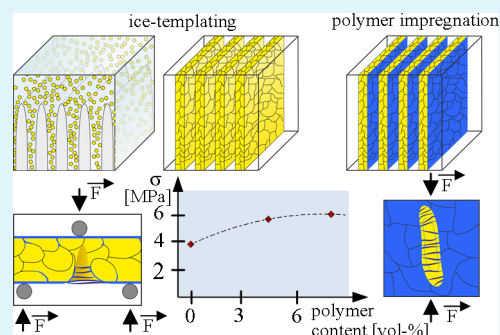
1. INTRODUCTION

In recent years the ice-templating process has been established as a suitable process to produce porous materials with open and aligned porosity and controllable microstructure.[1] Ice-templated scaffolds have demonstrated their suitability to serve as a bone replacement material.[2,3] It was also shown that dense composites that base on ice-templated scaffolds exhibit impressive properties in terms of toughness and strength.[4−7] These ice-templated composites seem to be a key for the design of bioinspired hierarchic materials. They show similarities with the hierarchical hybrid structure of several biominerals like nacre, trabecular bone and antler. Beyond that, they are capable of utilizing some of the failure mechanisms of biological hybrid materials. In a previous study we have investigated the structural and mechanical properties of pure β-tricalcium phosphate (β-TCP) scaffolds prepared by the ice-templating process.[8] Although we succeeded in preparing bioresorbable β-TCP scaffolds with structural sizes, porosities, and strengths similar to trabecular bone, the scaffolds were very brittle. The main limitation of calcium phosphates (CaP) for the replacement of bone seems not to be related to their strength but to their toughness and reliability.[9] The infiltration of ice-templated porous hydroxyapatite with gelatin and a subsequent cross-linking of the gelatin was demonstrated as a path to fabricate porous composites with increased strength and modulus.[10] However, it was also shown that the toughness of

alumina[11] and CaP[12] scaffolds can be significantly increased by the infiltration with the bioresorbable Thermoplast poly(ε-caprolactone) (PCL). This polymer forms fibrils during scaffold rupture and therefore increases the energy consumption during failure. It was also shown that the strength and toughness of robocast β-TCP scaffolds can be enhanced by a complete infiltration with PCL or polylactid acid (PLA).[13,14] The robocast scaffolds exhibit a macroporous structure build up by ceramic rods. The rods themselves exhibit micropores. The increase in strength was explained by "defect healing" due to the impregnation of the micropores by the polymer and by a stress shielding effect of the polymer that completely fills the macropores.[13,14] The "defect healing" hypothesis assumes that preexisting flaws can be healed by the impregnating polymer. Consequently, the healing of flaws increases the stress that is necessary to initiate the propagation of a crack starting from a defect.[13−15] The stress shielding mechanism was explained and simulated for the completely infiltrated scaffolds and is directly linked to the impregnation with a polymer of comparatively high modulus of elasticity like PLA.[13] Recently, it was also shown that an enhancement of strength, toughness, and reliability of robocast β-TCP scaffolds is possible by a PCL

Table 1. Summary of Processing Conditions, Initial Properties, and Testing Methods

onset ice front velocity	initial solid content (vol %)	initial sintered porosity (%)	PCL content (vol %) of the composite			mechanical testing
20 μm/s	20	68.6 ± 1.8	0		4.3	7.6	3-point flexural
20 μm/s	20	66.5 ± 1.4	0	0.7	4.4	7.6	
	10	85.6 ± 0.6	0		3.8		
30 μm/s	20	65.8 ± 1.0	0		4.7		compression
	30	50.1 ± 1.5	0		4.6		

coating process where the macroporous structure of the scaffolds was preserved.[15]

The objective of the present study is to improve the mechanical properties of ice-templated β-TCP scaffolds by a solution-mediated PCL impregnation. Here, we demonstrate the fabrication of porous composite scaffolds based on ice-templated sintered and bioresorbable ceramic scaffolds. For this purpose we intended to add the PCL polymer at an amount small enough to impregnate the micropores of the β-TCP scaffolds and to preserve the typical lamellar, open, and aligned macropores but high enough to enhance the mechanical properties regarding strength and toughness.

2. EXPERIMENTAL SECTION

2.1. Scaffold Preparation. The β-TCP scaffolds were fabricated by an ice-templating process that was described in detail previously.[8] Phase-pure β-TCP powder with a Brunauer−Emmett−Teller surface of 8 m^2/g and an average Feret diameter of 0.3 μm was used to prepare water-based suspensions with a solid content of 10, 20, and 30 vol %, respectively. Poly(vinyl alcohol) (1 wt % of the dry powder mass, 22 000 g/mol, ≥98%, VWR) and poly(acrylic acid) (1 wt % of the dry powder mass, 56 220 g/mol, Dolapix PC 21, Zschimmer and Schwarz, Germany) were added as binder and dispersant, respectively. The mixture was stirred in an ultrasonic bath for 10 min. Subsequently, it was degassed to achieve homogeneous slurries free of bubbles. The suspensions were cooled to approximately 0 °C and frozen unidirectional by utilizing onset ice front velocities of 20 and 30 μm/s, respectively. Two different casting molds were used to achieve cylindrical (mold with 14 mm diameter) and cuboid-shaped (mold with square cross section and 8 mm side length) samples. The frozen slurries were freeze-dried for at least 48 h at 103 Pa and 20 °C (ALPHA 2-4 LSC, CHRIST, Germany). The binder and dispersant were burned out for 30 min at constant temperatures of 400 and 500 °C, respectively. The heating rate was 10 K/min. Subsequently, the temperature was increased to 1100 °C with a rate of 10 K/min, and the scaffolds were sintered for 150 min. The sintered scaffolds with aligned and open porosity were cut to cylinders (10 mm height, 11 mm diameter) and beams (25 mm length, 6 mm width, 3 mm height) for compression and 3-point bending tests, respectively. All test specimens were cut at a minimum distance of 2 mm to the cooling finger to ensure the removal of the disturbed initial zone.[8]

2.2. Polymer Infiltration. The semicrystalline Thermoplast PCL with a mass average molecular weight (M_w) of 50 000 g/mol, a glass transition temperature of −60 °C, a melting temperature of 60 °C, and an elongation at break of 800% (Capa 6500, Perstorp, U.K.) was dissolved in acetone (>98.5%, Carl Roth) and stirred for 120 min to achieve a homogeneous solution. The sintered scaffolds were immersed in PCL solutions with 1.5 and 5 wt % PCL content, respectively. For this purpose the scaffolds were slowly dipped into the solution where they remained for 3 min. Subsequently, they were dried for 30 min at room temperature using a desiccator. Repeating the infiltration step several times led to composite samples with higher polymer content. After infiltration all samples were heat treated at 160 °C for 30 min to remove residual acetone and to homogenize the polymer film on the lamellae surface and in the micropores of the scaffold. In a first series of experiments the applicability of the impregnation process and its influence on the mechanical properties were tested with scaffolds prepared with 20 vol % initial solid content

and 20 μm/s onset ice front velocity. Cylindrical samples were designated for compression tests, and 16 samples of one batch were divided into four fractions. The first fraction was not infiltrated, and the other three fractions were immersed one time in 1.5 wt % PCL solution, two times in 5 wt % PCL solution, and four times in 5 wt % PCL solution, respectively. This corresponds to final PCL content in the composite scaffolds of 0 vol %, 0.7 ± 0.1 vol %, 4.4 ± 0.1 vol %, and 7.6 ± 0.1 vol %, respectively. Twelve beam samples designated for flexural tests were also split in three fractions. These fractions of beams were not infiltrated, immersed two times, and immersed four times in 5 wt % PCL solution, which correspond to composite scaffolds with 0 vol %, 4.3 ± 0.1 vol %, and 7.6 ± 0.2 vol % PCL content, respectively. On the basis of these impregnation tests a PCL content of ∼4 vol % was selected for all further experiments. The influence of a 4 vol % PCL impregnation on the mechanical properties of composite scaffolds was investigated using β-TCP scaffolds that were fabricated with 30 μm/s onset ice front velocity and three different solid contents (10, 20, and 30 vol %), that is, three different porosities (Table 1). For this purpose seven cylindrical samples per batch were immersed two times in 5 wt % PCL solution.

2.3. Morphological Characterization. The sintered β-TCP scaffolds were infiltrated with an epoxy (SpeciFix, Stuers, Germany) and sectioned. Longitudinal sections and cross sections were examined by light microscopy (Axio Imager M2m, Carl Zeiss, Germany) and SEM (S440i, Leica, Germany). Pore widths and ceramic lamella thicknesses were measured in cross section. To determine structural sizes three different images at one cross sectional position were taken. A minimum of 100 values for each image of one cross sectional position were measured and the mean as well as the standard deviation were calculated. The β-TCP/PCL composites were examined by SEM after mechanical testing (fracture surfaces, debris). The porosity of the samples were determined by measuring mass and volume before and after PCL infiltration (ρ_{TCP} = 3.07 g/cm^3, ρ_{PCL} = 1.10 g/cm^3).

2.4. Mechanical Characterization. The mechanical properties were characterized using a static materials testing device (Zwick/Roell Z020, Zwick, Germany). The compression and three-point flexural tests were performed with a constant crosshead speed of 5 mm/min. The three-point flexural tests were performed using beam specimens. A support distance of 16 mm was chosen, and the alignment of pores and ceramic lamellae were perpendicular to the applied load. The compression tests were performed by using cylindrical samples. The load was applied parallel to the alignment of pores and β-TCP lamellae. The mechanical tests were filmed with a digital reflex camera (Canon Inc., Japan).

For all strength measurements of the samples summarized in Table 1 the arithmetical means and standard deviations were calculated. Because of the restricted amount of tested specimens a parameter estimation was performed to determine the confidence intervals for the true means of the flexural and compression strength values. For the parameter estimation a normal distribution of the unknown means and their unknown variance was assumed. Hence, a test statistic was computed, which is described by the Student's t-distribution. In this manner the intervals were calculated, which include the true means at a 95% level of confidence.

3. RESULTS

3.1. Scaffold Morphology. The pure ceramic β-TCP scaffolds as well as β-TCP/PCL composite scaffolds show the typical morphology known for ice-templated ceramic suspen-

846

dx.doi.org/10.1021/am507333q | ACS Appl. Mater. Interfaces 2015, 7, 845−851

sions (Figure 1). The pores are aligned and continuously connected from the bottom to the top of the sample in their
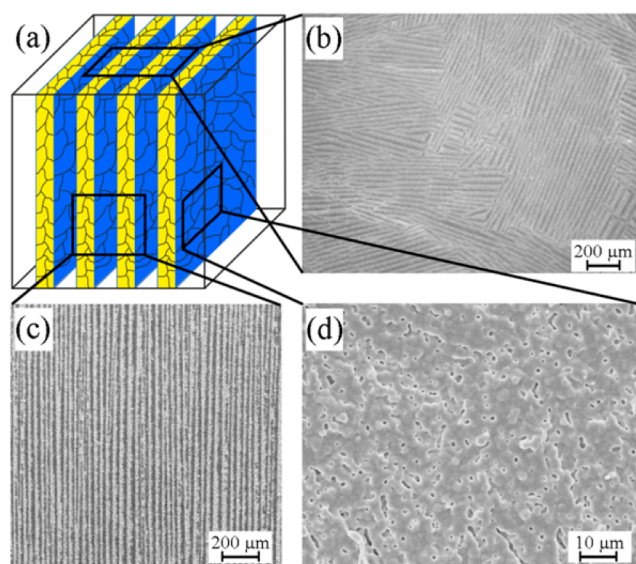

Figure 1. Scaffold morphology: (a) scheme of a composite scaffold with the β-TCP ceramic lamellae (yellow) and the PCL film on the lamellae (blue), (b) cross section of lamellar domains with a random orientation to each other, (c) longitudinal section of aligned lamellar pores and ceramic, (d) surface of a lamella illustrating the residual porosity before infiltration. Dark regions represent the pores, and bright regions represent the β-TCP ceramic.

longitudinal section (Figure 1c). In the cross section the pores and the ceramic β-TCP lamellae are arranged in domains with a random orientation to each other (Figure 1b). The influence of the solid content in the suspension as well as of the onset ice front velocity on the structure and properties of ice-templated pure β-TCP scaffolds was already investigated in a previous study.[8] Increasing the ice front velocity at a constant solid content does not affect the porosity of the scaffolds but decreases their structural sizes and consequently increases their strength. Each ceramic β-TCP lamella exhibits a distinct microporosity (Figure 1d). During the PCL impregnation these micropores are filled with PCL. Additionally, the surfaces of the lamellae as well as cracks located at these surfaces are coated with a thin PCL film. The structural sizes of the scaffolds used in this work are summarized in Table 2.

Table 2. Structural Sizes of Sintered β-TCP Scaffolds in Dependence on the Processing Parameters Initial Solid Content of the Suspension and Onset Ice Front Velocity

solid content (vol %)	20	10	20	30
velocity (μm/s)	20	30	30	30
pore width (μm)	20 ± 4	15 ± 3	12 ± 3	8 ± 3
ceramic lamellae thickness (μm)	15 ± 4	5 ± 1	11 ± 3	13 ± 3

3.2. Mechanical Properties. *3.2.1. Damage-Tolerant Behavior of Composite Scaffolds.* Figure 2 shows flexural stress-deflection curves and compressive stress−strain curves of pure ceramic and composite scaffolds. The impregnation of β-TCP scaffolds with PCL leads to a composite scaffold with increased energy consumption during failure under compression and bending load. The areas under the stress−deflection

and stress−strain curves indicate the amount of energy consumption. In both cases this energy considerably increases with the PCL addition. The overall scaffold characteristic changes from the brittle performance of pure ceramic scaffolds to a more plastic behavior of the composites. In contrast to the pure β-TCP scaffolds the composite scaffolds still stick together after the scaffold collapses. Furthermore, they are able to bear load and consume mechanical energy during further bending (Figure 2a) or compression (Figure 2b). This kind of damage-tolerant behavior is also illustrated in the Supporting Information, movies sm1 and sm2. Movie sm1 compares the compression of a ceramic scaffold and a PCL-impregnated scaffold. After the first rupture the pure ceramic scaffold falls into pieces and forms a lot of debris, whereas the composite scaffold remains intact even at high loads (movie sm1). Movie sm2 shows a representative three-point flexural test of a composite scaffold, which illustrates the storage of elastic energy within the scaffold after load retraction (movie sm2).

3.2.2. Compressive and Flexural Strength of Ice-Templated β-TCP and β-TCP/PCL Scaffolds. Samples prepared with an initial solid content of 20 vol % and an onset ice front velocity of 20 μm/s show an increase in flexural and compression strength after PCL impregnation (Figure 3). The flexural strength increases from 3.4 to 5.3 and 5.6 MPa when PCL was added at an amount of 4.2 vol % and 7.6 vol %, respectively. The compressive strength increases from 4.4 to 6.0 MPa, 9.5 and 10.3 MPa when PCL was added at an amount of 0.7 vol %, 4.4 vol %, or 7.6 vol %, respectively The purpose of enhancing the mechanical properties at a minimum amount of PCL addition was found to be in the region of 4 vol % PCL content. An increase of the PCL content to 7.6 vol % does not significantly induce a pursued strength increase.

However, the strength increase at a given PCL content also depends on the initial solid content, which affects the scaffold porosity, microstructure, and initial scaffold strength. At a PCL content of approximately 4 vol % scaffolds with initial porosities of 85.6% and 65.8% show a significant increase of their compressive strength from 0.8 to 1.4 MPa and from 12.5 to 17.7 MPa, respectively (Figure 4a,b). On the other hand, at an initial porosity of only 50.1%, which corresponds to the highest initial scaffold strength, the PCL impregnation doesn't contribute to a significant strength increase (Figure 4c). For these samples the polymer impregnation only improves the damage tolerance.

3.3. Microscopic Analysis of Fractured Composite Scaffolds. After crack initiation and crack extension fractured scaffolds exhibit PCL fibers bridging the cracks. This is independent of the mechanism of the crack formation, which occurred either by bending (Figure 5b) or by compression load (Figure 6). A failure under compression load leads to several adjacent microcracks within the TCP lamella, which are bridged by PCL fibrils (Figure 6). The PCL fibers do not only span microscopic cracks but also bridge larger sample separations as shown for a bending beam after failure (Figure 5a). Hence, the ceramic debris is still glued together after failure of the ceramic and remains arranged close to the initial array.

4. DISCUSSION

The objective of this study was to enhance the mechanical properties of ice-templated ceramic scaffolds by a polymer impregnation. The results have shown that it is possible to alter the mechanical properties and fracture behavior of PCL-impregnated β-TCP scaffolds without changing their macro-
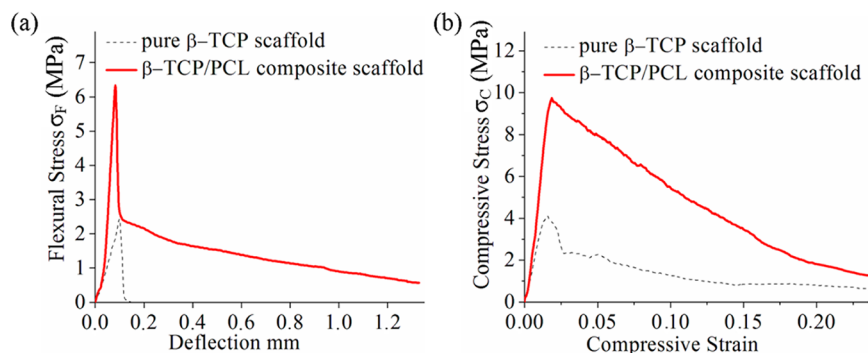
Figure 2. Comparison of the mechanical behavior of pure ceramic β-TCP scaffolds and PCL-impregnated composite scaffolds fabricated with an onset ice front velocity of 20 μm/s and an initial solid content of 20 vol %: (a) flexural stress-deflection curves of a pure ceramic scaffold and a composite scaffold with 4.3 vol % PCL, (b) compression stress−strain curves of a pure ceramic scaffold and a composite scaffold with 4.4 vol % PCL.
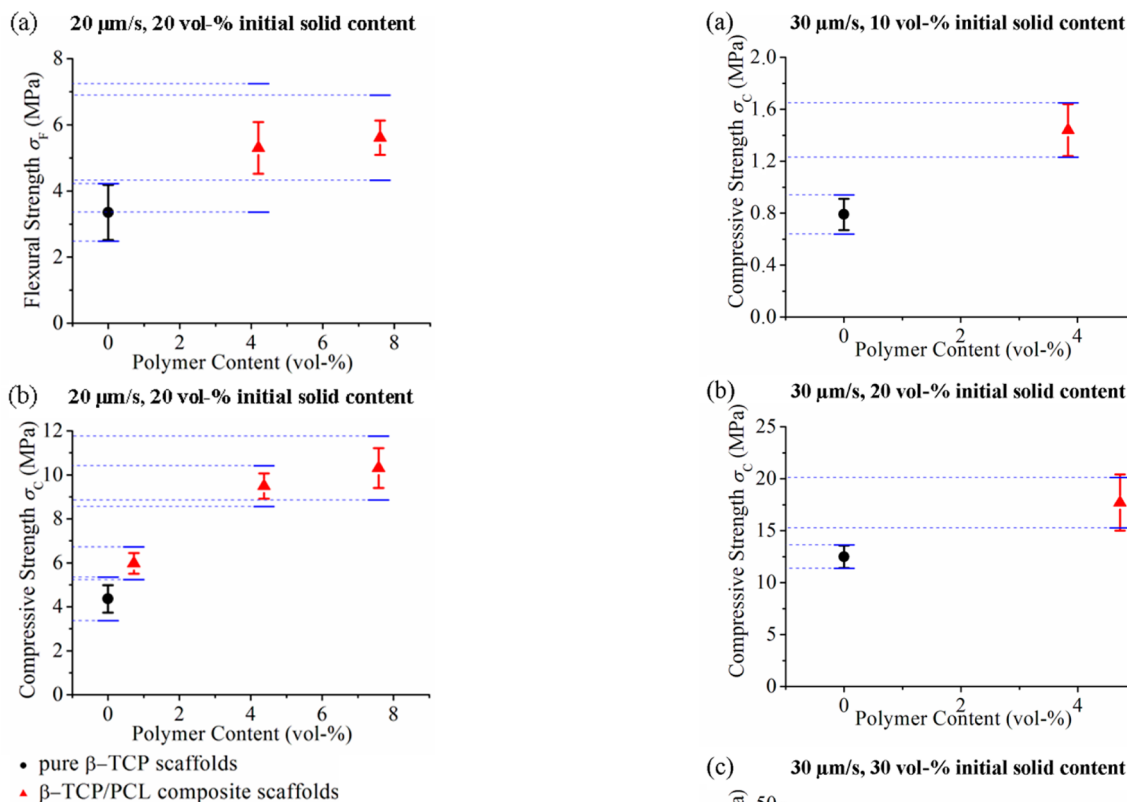

Figure 3. Influence of the PCL content on the scaffold strengths for samples prepared with an onset ice front velocity of 20 μm/s and an initial solid content of 20 vol %: (a) flexural strengths, (b) compressive strengths. The blue dashed lines and bars represent the interval where the true value of the mean strength is found with a 95% level of confidence.

porous structure. The composite scaffolds exhibit enhanced damage tolerance that results from the elevated energy consumption during failure, a change in the failure mechanism, and increased compression and flexural strengths.

Initially it seems astonishing that the impregnation of lamellae of a stiff and strong ceramic material like β-TCP (bulk material modulus of elasticity: 33 GPa measured,[16] 110 GPa calculated;[17] bulk material tensile strength: 140 MPa[16]) by a ductile polymer like PCL (modulus of elasticity: 0.53 GPa[13]) leads to a strength increase. Our observations reveal that PCL fibrils emerge during crack extension (Figure 6). Our hypothesis assumes that the strength increase is induced by a
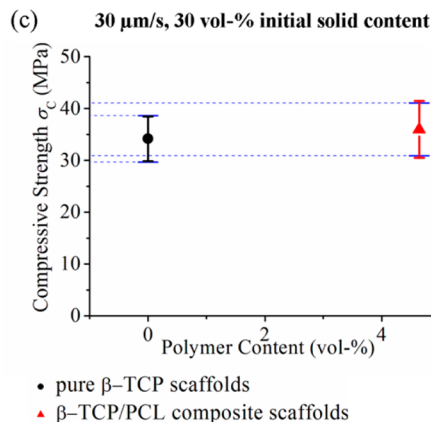

Figure 4. Influence of a 4 vol % PCL addition on the compressive strengths of β-TCP scaffolds fabricated with an onset ice front velocity of 30 μm/s. The initial porosity of sintered samples was (a) 85.9%, (b) 65.8%, and (c) 50.1%. The blue dashed lines and bars represent the interval where the true value of the mean strength is found with a 95% level of confidence.
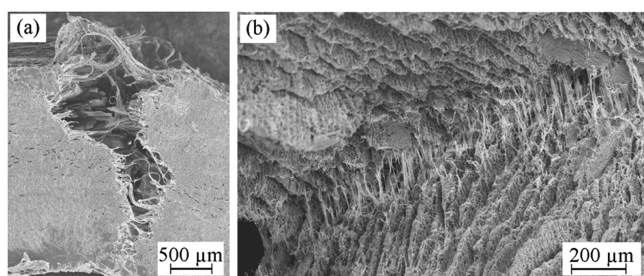
Figure 5. (a) SEM image of a bending beam after failure and (b) insight into the macroscopic main crack where the extension is impended by PCL.
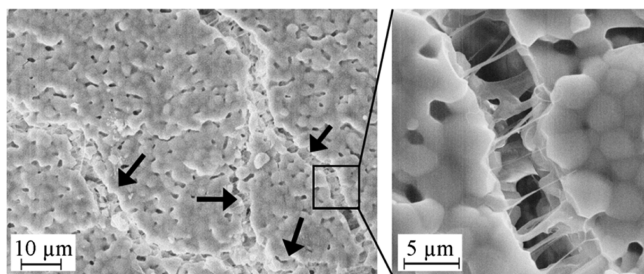

Figure 6. SEM images of elongated cracks within a β-TCP lamella after failure under compression, showing the bridging of PCL fibers and the branching of cracks (black arrows—multiple cracks).

Figure 7. Scheme of the failure mechanism of the composite scaffolds under (a) bending mode and (b) compression mode. PCL (blue) present on the surface and inside surface flaws and micropores of the β-TCP lamellae (yellow) forms fibers during crack extension. The PCL is cold drawn to fibers during the crack growth and crack extension. The cold-drawn fibers with increased strength and modulus of elasticity bridge the crack and transfer load across the crack. Fibrils also glue the scaffold together even after failure of the ceramic lamellae.

stiffening mechanism that is based on the cold drawing and strain hardening of the PCL thermoplastic during crack extension and opening. Cold-drawn polymers can show strain hardening under tension load if a stable necking developed after stretching.[18] When the deformation proceeds, morphological changes (e.g., strain-induced crystallization) and the orientation of molecular chains parallel to the tensile load axis lead to increased strength values and to an increasing strain-hardening modulus.[19−21] The formation of microfibrils with higher moduli of elasticity and higher tensile strengths was also observed for polyethylene where high drawing ratios led to oriented and taut-tied molecules.[22] The mechanism of cold drawing has also been reported for PCL (M_w = 115 000 g/mol) where a fiber elongation of 500% leads to a 5-fold increase of the tensile strength (from 8 to 43 MPa) and a 3-fold increase of the elastic modulus (from 0.1 to 0.3 GPa).[23] In our proposed explanatory model PCL fills the accessible micropores and the surface flaws of lamellae (Figure 7). If a load is applied to the sample by bending (Figure 7a) or compression (Figure 7b), stress develops inside the ceramic lamellae, and stress concentrations are located in the vicinity of surface flaws and micropores. Because of these stress concentrations cracks start to propagate. With the extension of cracks, the PCL inside the opened micropores is drawn to fibrils that bridge the cracks. At small crack extensions these fibrils only contribute to the increased energy consumption during deformation. At larger crack extensions the fibrils reach a level where a significant drawing and strain-hardening effect leads to stiff and strong fibers that are able to transfer an appreciable amount of load across the crack gaps (Figure 7). It may be assumed that the strength and modulus of the β-TCP lamellae are significantly below the above-mentioned values due to the residual pores.[24−26] Hence, the values are in a range comparable to the strain-hardened PCL fibers. As the PCL fibrils transfer load across the crack flanks, the stress at the crack tip is decreased. Consequently, a
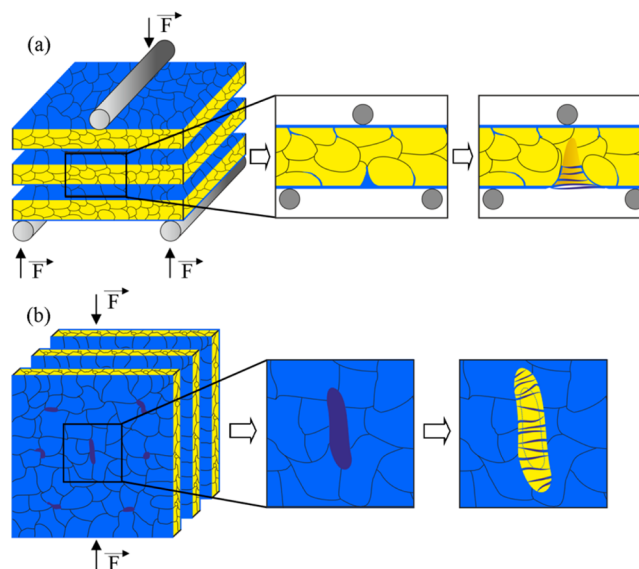
higher macroscopic load is required to achieve further crack growth. This leads to the higher strengths of composite scaffolds compared to pure β-TCP scaffolds because an even higher load is necessary to provoke crack propagation and catastrophic failure.

The stiffening of PCL fibers can only occur if the polymer is extended to an appropriate degree. At the same time the crack must be in a stable propagation mode, and the ceramic may not yet have failed completely. If the initial scaffold strength is too high, as in the case for structures with a low porosity, the aforementioned assumptions are not valid, and a strength enhancement by PCL impregnation is not possible (Figure 4c). Hence, the mechanism only occurs for material combinations where the cold-drawn polymer and the porous ceramic have similar mechanical properties and where open micropores allow the polymer impregnation.

Increasing the PCL content above approximately 4 vol % does not contribute to a further significant strength increase. It is assumed that around this PCL content a sufficient PCL film thickness is achieved to fill surface flaws and micropores. Though further PCL addition increases the PCL film thickness, the contribution to the strength increase by cold-drawn fibrils is restricted. The degree of drawing and therefore the degree of strength increase of the oriented fibers depends on the polymer extension. The PCL extension is spatio-dependent and limited to the vicinity of cracks and micropores (Figure 8). This explanatory model for strength increase requires an initial crack extension level to be valid. In contrast to this, a model proposed by Martínez-Vázquez et al. assumes a healing of surface defects by the PCL impregnation. This leads to higher stresses that are necessary to initiate crack propagation from the filled defects. Therefore, cracks will have to start from completely different flaws.[13−15] However, in our case the initial bulk mechanical

849

dx.doi.org/10.1021/am507333q | ACS Appl. Mater. Interfaces 2015, 7, 845−851
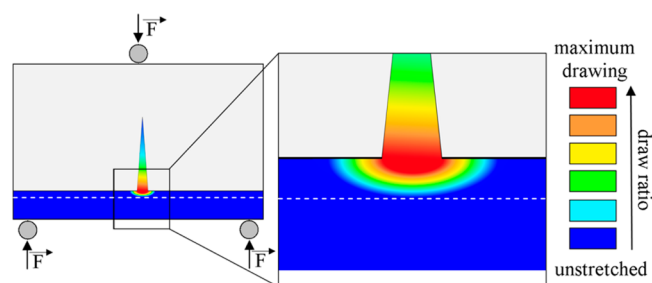
Figure 8. Scheme of the relative distribution of the PCL draw ratio within a crack. The PCL film won't be drawn to an appreciable amount above a certain level of thickness that is restricted by the white dashed line. Therefore, additional PCL material above this thickness won't contribute to a further strength increase by strain hardening.

properties of PCL and β-TCP are too different to complement one another.

The strength increase contributes only to a small degree to the improved damage tolerance of the composite scaffolds. Instead, altered failure mechanisms and elevated energy consumption during failure must be taken into account. The failure mechanism changes from a pure brittle behavior to a deformation behavior with brittle as well as plastic contributions. In particular, this is apparent for scaffolds under bending load. Pure ceramic scaffolds fail in a brittle manner and are not able to bear any load after an initial failure (Figure 2a, dashed line). On the other hand the composite scaffolds are capable to bear load even after their initial failure and further deflection (Figure 2a, continuous line). This behavior can be directly correlated to the bridging of cracks and large material separations (Figure 5a,b). The increased energy consumption during failure can be explained by four factors:

(i) The additional elastic and plastic energy consumption generated by the introduced PCL.

(ii) The friction of glued scaffold debris, which occurs in particular under compression load.

(iii) The PCL fibril formation increases the crack extension resistance by bridging micro- and macrocracks. This is comparable to extrinsic toughening mechanisms where the toughness is developed during crack extension.[27]

(iv) The formation of several adjacent and branched cracks under compression load that are bridged by PCL fibrils (Figure 6). In agreement with results found for engineered cementitious composites this could be derived by allowing cracks to grow from pre-existing flaws in a controlled manner leading to a large number of closely spaced microcracks.[28,29] In the case of ice-templated scaffolds the propagation of larger cracks seems to be impeded, and smaller adjacent cracks or even new cracks start to grow.

5. CONCLUSIONS

Damage-tolerant β-TCP scaffolds with significantly increased compression and flexural strengths were prepared by ice-templating and a subsequent PCL impregnation. The strength increase of impregnated scaffolds mainly results from the stiffening of cold-drawn and strain-hardened PCL fibers formed after crack initiation and crack extension. The increased energy consumption of composite scaffolds during scaffold failure is related to an extrinsic toughening mechanism. The PCL impregnation of ice-templated β-TCP scaffolds seems to be a

promising pathway to produce bioresorbable bone replacement materials with adjustable porosities, pore sizes, and mechanical properties. Because of their damage tolerance these materials could be of particular interest to design novel implant architectures for load-bearing applications.

■ ASSOCIATED CONTENT

ⓢ Supporting Information

Demonstrations of the different failure of a ceramic β-TCP scaffold and a composite β-TCP/PCL scaffold under compression load (movie sm1) and the failure of a composite scaffold in a three-point flexural test (movie sm2). This material is available free of charge via the Internet at http://pubs.acs.org.

■ AUTHOR INFORMATION

Corresponding Author
*Phone: +493641947765. Fax: +493641947702. E-mail: stefan.flauder@uni-jena.de.

Notes
The authors declare no competing financial interest.

■ ACKNOWLEDGMENTS

■ REFERENCES

(1) Deville, S. Freeze-Casting of Porous Ceramics: A Review of Current Achievements and Issues. *Adv. Eng. Mater.* **2008**, *10*, 155−169.

(2) Deville, S.; Saiz, E.; Tomsia, A. P. Freeze Casting of Hydroxyapatite Scaffolds for Bone Tissue Engineering. *Biomaterials* **2006**, *27*, 5480−5489.

(3) Iwasashi, M.; Muramatsu, T.; Sakane, M. Radiological and Histological Evaluation of Regenos® Which Implanted in Human Radial Fracture: A Clinical Case Report. *Key Eng. Mater.* **2013**, *529−530*, 313−316.

(4) Deville, S.; Saiz, E.; Nalla, R. K.; Tomsia, A. P. Freezing as a Path to Build Complex Composites. *Science* **2006**, *311*, 515−518.

(5) Munch, E.; Launey, M. E.; Alsem, D. H.; Saiz, E.; Tomsia, A. P.; Ritchie, R. O. Tough, Bio-Inspired Hybrid Materials. *Science* **2008**, *322*, 1516−1520.

(6) Launey, M. E.; Munch, E.; Alsem, D. H.; Barth, H. B.; Saiz, E.; Tomsia, A. P.; Ritchie, R. O. Designing Highly Toughened Hybrid Composites Through Nature-Inspired Hierarchical Complexity. *Acta Mater.* **2009**, *57*, 2919−2932.

(7) Bouville, F.; Maire, E.; Meille, S.; Van de Moortèle, B.; Stevenson, A. J.; Deville, S. Strong, Tough and Stiff Bioinspired Ceramics from Brittle Constituents. *Nat. Mater.* **2014**, *13*, 508−514.

(8) Flauder, S.; Gbureck, U.; Müller, F. A. Structure and Mechanical Properties of β-TCP Scaffolds Prepared by Ice-Templating with Preset Ice Front Velocities. *Acta Biomater.* **2014**, *10*, 5148−5155.

(9) Wagoner Johnson, A. J.; Herschler, B. A. A Review of the Mechanical Behavior of CaP and CaP/Polymer Composites for Applications in Bone Replacement and Repair. *Acta Biomater.* **2011**, *7*, 16−30.

(10) Landi, E.; Valentini, F.; Tampieri, A. Porous Hydroxyapatite/Gelatine Scaffolds with Ice-Designed Channel-Like Porosity for Biomedical Applications. *Acta Biomater.* **2014**, *4*, 1620−1626.

(11) Peroglio, M.; Gremillard, L.; Chevalier, J.; Chazeau, L.; Gauthier, C.; Hamaide, T. Toughening of Bio-Ceramics Scaffolds by Polymer Coating. *J. Eur. Ceram. Soc.* **2007**, *27*, 2679−2685.

(12) Peroglio, M.; Gremillard, L.; Gauthier, C.; Chazeau, L.; Verrier, S.; Alini, M.; Chevalier, J. Mechanical Properties and Cytocompatibility of Poly(ε-caprolactone)-Infiltrated Biphasic Calcium Phosphate

Scaffolds with Bimodal Pore Distribution. *Acta Biomater.* **2010**, *6*, 4369−4379.

(13) Martínez-Vázquez, F. J.; Perera, F. H.; Miranda, P.; Pajares, A.; Guiberteau, F. Improving the Compressive Strength of Bioceramic Robocast Scaffolds by Polymer Infiltration. *Acta Biomater.* **2010**, *6*, 4361−4368.

(14) Martínez-Vázquez, F. J.; Perera, F. H.; van der Meulen, I.; Heise, A.; Pajares, A.; Miranda, P. Impregnation of β-Tricalcium Phosphate Robocast Scaffolds by in situ Polymerization. *J. Biomed. Mater. Res., Part A* **2013**, *101A*, 3086−3096.

(15) Martínez-Vázquez, F. J.; Miranda, P.; Guiberteau, F.; Pajares, A. Reinforcing Bioceramic Scaffolds with in situ Synthesized ε-Polycaprolactone Coatings. *J. Biomed. Mater. Res., Part A* **2013**, *101A*, 3551−3559.

(16) Jarcho, M.; Salsbury, R. L.; Thomas, M. B.; Doremus, R. H. Synthesis and Fabrication of β-Tricalcium Phosphate (Whitlockite) Ceramics for Potential Prosthetic Applications. *J. Mater. Sci.* **1979**, *14*, 142−150.

(17) Liang, L.; Rulis, P.; Ching, W. Y. Mechanical Properties, Electronic Structure and Bonding of α- and β-Tricalcium Phosphates with Surface Characterization. *Acta Biomater.* **2010**, *6*, 3763−3771.

(18) Ward, I. M.; Sweeney, J. In *An Introduction to the Mechanical Properties of Solid Polymers;* Wiley: New York, 2004; Chapter 11, pp 241−270.

(19) Jäckel, K. Ein Beitrag zur Kaltverstreckung der Hochpolymeren. *Colloid Polym. Sci.* **1954**, *137*, 130−162.

(20) Lazurkin, J. S. Cold-Drawing of Glass-Like and Crystalline Polymers. *J. Polym. Sci.* **1958**, *30*, 595−604.

(21) Ting, G. E.; Robbins, M. O. Anisotropic Plasticity and Chain Orientation in Polymer Glasses. *J. Polym. Sci., Part B: Polym. Phys.* **2010**, *48*, 1473−1482.

(22) Meinel, G.; Peterlin, A. Plastic Deformation of Polyethylene II. Change of Mechanical Properties During Drawing. *J. Polym. Sci., Polym. Phys. Ed.* **1971**, *9*, 67−83.

(23) Williamson, M. R.; Adams, E. F.; Coombes, A. G. A. Gravity Spun Polycaprolactone Fibres for Soft Tissue Engineering: Interaction with Fibroblasts and Myoblasts in cell Culture. *Biomaterials* **2006**, *27*, 1019−1026.

(24) Knudsen, F. P. Dependence of Mechanical Strength of Brittle Polycrystalline Specimens on Porosity and Grain Size. *J. Am. Ceram. Soc.* **1959**, *42*, 376−387.

(25) Rice, R. W. Comparison of Stress Concentration Versus Minimum Solid Area Based Mechanical Property-Porosity Relations. *J. Mater. Sci.* **1993**, *28*, 2187−2190.

(26) Rice, R. W. Comparison of Physical Property-Porosity Behaviour with Minimum Solid Area Models. *J. Mater. Sci.* **1996**, *31*, 1509−1528.

(27) Launey, M. E.; Ritchie, R. O. On the Fracture Toughness of Advanced Materials. *Adv. Mater.* **2009**, *21*, 2103−2110.

(28) Li, V. C. On Engineered Cementitious Composites (ECC): A Review of the Material and its Applications. *J. Adv. Concr. Technol.* **2003**, *1*, 215−230.

(29) Li, V. C. Tailoring ECC for Special Attributes: A Review. *Int. J. Concr. Struct. Mater.* **2012**, *6*, 135−144.